CONTRAST ENHANCEMENT CALCULATION OF X-RAY IMAGING

Togtokhtur T.[a,b1], *Dushanov E.B.*[a,c], *Batmunkh M.*[a], *Bugay A.N.*[a,c]

[a] Laboratory of Radiation Biology, JINR, Dubna, Russia

[b] Institute of Physics and Technology, Mongolian Academy of Science, Mongolia

[c] Dubna State University, Dubna, Russia

Abstract – A computed tomography (CT) scan has been improved to clarify a tumor sites and size by utilizing radiocontrast media in medical X-ray imaging techniques. In particular, well-tolerated contrast images of a phantom containing mixtures of contrast agents such as iodine and gadolinium have absorbed the photons high. In this work, the effect of a two-dimensional projection image of an imaging phantom adapted to a preclinical experimental setup containing mixtures of contrast agents depending on their concentration, distribution and materials was evaluated using the Monte Carlo method. The projection image produced from the calculation demonstrated different tolerances for each iodine concentration, and the brightest part corresponded to the rod with the highest concentration. However, it could not be demonstrated well in the shorter targets. Nevertheless, the image tolerance on the target with the iodinated shell was brighter than the uniform distribution due to increased iodine volume density. As a result, the calculation could be given to find the optimal distribution of the iodine in biological objects for X-ray imaging. Finally, this study indicates the perspective of enhanced CT on targeted sites of imaging phantom-filled soft tissue (ICRP) at potential concentrations within a safe range of iodine without difficulty.

PACS: 87.53.-j, 87.19.xj, 87.59.Fm

INTRODUCTION

X-ray tubes used in clinical CT energy range from 80 to 150 kVp. They not have been clarifying well image quality if considering the pathological differences of elemental composition of materials are very slight [1, 2]. Common indications for contrast media (CM) include inflammatory, malignant or neoplastic conditions, and CM is substance used to improve pictures of inside parts of the body produced by X-rays. Commonly, iodine is low K-edge 33.1 keV metallic element that adaptable for common X-ray imaging. Contrast effect has more effective when using higher voltage X-ray tube. Notably, it mentioned that iodinated contrast media (ICM) is mostly non-ionic and available for biological objects [3, 4]. The most ICM is available preclinical CT, their contrast Hounsfield units (HU) value has been reached iodine at the 8.75 mg/mL [5]. The recent article has reported safe waiting intervals between successive contrast-enhanced imaging studies with iodine-based CM, gadolinium-based contrast agents (GBCA), or a combination of both [6]. In last decade, Monte-Carlo method has been applied to improve and predict

[1] E-mail: togtokhtur@jinr.ru

advances in CT [7]. Here, we present an estimation radio-enhancement effect of X-ray imaging on the soft tissue (ICRP) [8] phantom containing pure iodine and gadolinium agents and our obtained results in two different scenarios.

1. MATERIALS AND METHODS

1.1. GEANT4 low energy EM physics. GEANT4 Monte-Carlo code was used to model the imaging phantom exposed by X-ray irradiation. The Livermore cross section was used in this simulation, which includes processes like the photoelectric effect, Compton, and Rayleigh scattering. [9]. The model indicates the interaction of electrons and photons with matter down to 10 eV (cut-off energy).

1.2. The X-ray spectrum. The spectrum was generated by SpekPy software [10] based on physical model casim (PENELOPE data set) tube voltage 130 kVp [11] using inherent filtration of 0.8 mm beryllium and 3.9 mm of aluminum (HVL = 0.68 mm Cu) and used as an X-ray source in this simulation (see Fig. 1).

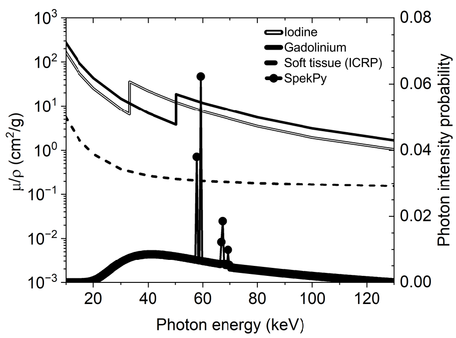

Fig. 1. Mass attenuation coefficient (primary Y-axis) and X-ray spectrum (secondary Y-axis) for the simulation study.

1.3. The mass attenuation coefficient. This quantity used materials in the simulation (μ/ρ) was defined using NISTX for distinction [12]. Where (μ/ρ) represents the mass attenuation coefficient, which describes the interaction probability of energetic photons with materials. It is higher for the metals compared to soft tissue (ICRP) with average percentage of elements (H-10.5%, C-25.6%, N-2.7%, O-60.2%, Na-0.1%, P-0.2%, S-0.3%, Cl-0.2%, K-0.2%), density of 1.0 g/cm^3 [8], as shown in the double, single, and dashed lines, respectively (Fig. 1). Also, it is related to the characteristic lines of the X-ray spectrum. High-voltage X-rays are more suitable for the radiocontrast effect. Hence, it requires an energy peak of tube spectrum higher than the metals K-edge considering that the emission of photoelectrons increases when using pure iodine and gadolinium compared with soft tissue (ICRP).

1.4. GEANT4 geometry. An imaging phantom is the optimal way to demonstrate the X-ray image (section 1.5) when using the X-ray beam parallel with the front surface (XY) of the object (Fig. 2). The following imaging

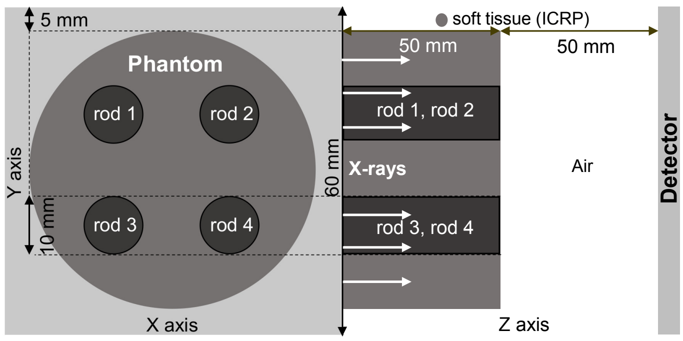

Fig. 2. The imaging phantom is illustrated in front (XY) and side (YZ) projection

phantom (Fig. 2) was designed using the experimental setup. The all geometries used in this simulation has built on the GEANT4 (see Fig. 2 and 3). The incident beam was traveling through phantom parallel (XY) and plane size (60 × 60 mm) same as CsI detector [11].

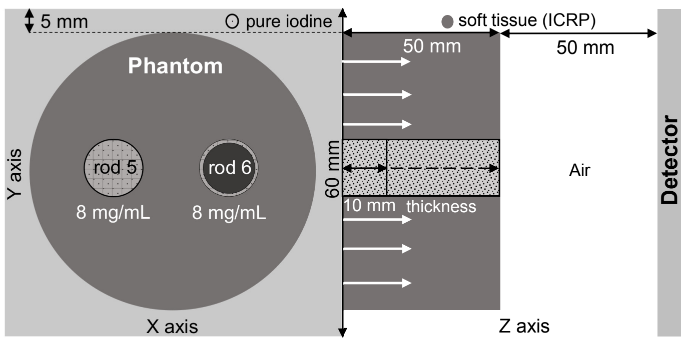

Fig. 3. The modified imaging phantom is illustrated in front and side projection.

The imaging phantom has been modified to have two rods for the purpose of identifying iodine contrast effects depending on their spread density and target thickness (Fig. 3). We have chosen shell accumulation that way in the rod 5 due to iodine could not be absorbed by every cell inside the tissue trail in some experiments. Here, we are assumed in comparing the contrast effect that depends on the iodine distribution with uniformly (rod 5) and the 0.1 mm thick shell (rod 6).

1.5. Simulation procedure. We estimated the photon count recorded at the detector following procedure. Here, notice that we did not consider the scintillation process of the photon inside the CsI detector due to some barrier with the code. At first, the (x, y) coordinates of the photons reaching the detector surface area passing through the imaging phantom are recorded in GEANT4. It means that the coordinates (points) obtained in every single step are collected as the signal on the detector. The obtained points were counted after making pixels 0.04 mm^2 in size using two-dimensional frequency estimation (heatmap) in the OriginPRO software (see Fig. 4 and 5); the color contrast depends on the frequency count (number of the points) for each pixel, and when the frequency count is higher, the pixels are darker. The optimal value of primary photon intensity at the beam source was $N_0 = 10^7$.

When $N_0 < 10^7$, X-ray images with poor tolerance (blurry) are mainly obtained, which is associated with a low pixel density. At $N_0 > 10^7$, the pixel density increases, and, accordingly, it takes quite a long time to form the required picture. The color scale bar was interpolated between the color site at 0 mg/ml (imaging phantom) concentration and the color site at 8 mg/ml concentration (Fig. 4 and 5). In each case of N_0, the average frequency count ratio for the imaging phantom and the brightest rod of the highest concentration is 1.525 ± 0.005; the color scale adjusted could not depend on the photon intensity.

2. RESULTS

2.1. The result images from the first stage of the simulation. In Fig. 4a, the contrast effect between rod 1 with iodine and rod 2 with gadolinium contrast media at 8 mg/mL along the mentioned model in Fig. 2 is shown. The contrast effect was very similar to each other for contrast agents due to either their K-edge energy being below the characteristic peak of the X-ray spectrum (Fig. 1). The projection image was calculated after uptake iodine at 2, 4, 6, and 8 mg/mL into the rods along clockwise (Fig. 4b). Particularly, the rod shape appeared applicable enough compared to soft tissue (ICRP) when 4 to 8 mg/mL iodine.

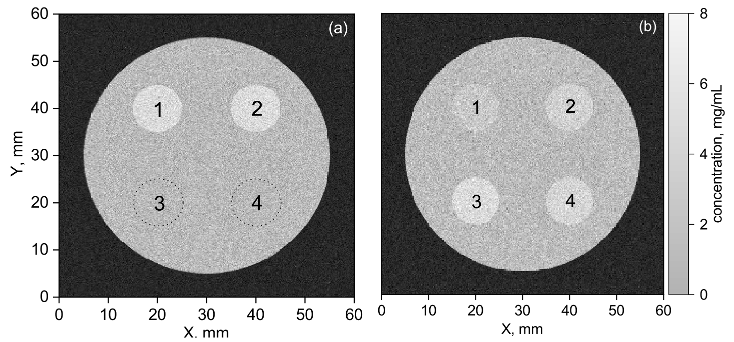

Fig. 4. X-ray images obtained for: (a) rod 1 (8 mg/mL iodine), rod 2 (8 mg/mL gadolinium), black dotted rods 3, 4 (0 mg/mL); (b) rod 1 (2 mg/mL iodine), rod 2 (4 mg/mL iodine), rod 3 (8 mg/mL iodine), rod 4 (6 mg/mL iodine).

2.2. The result images from the second stage of the simulation. Here are the images we obtained according to the previous geometry (see Fig. 3). The contrast effect significantly increased by the thickness of the rod 5 (Fig. 5). Because the photon fluence into the iodinated area decreased rapidly when material depth increases. Nevertheless, the effect slightly increased in the rod 6 with iodinated shell. Also, surface sharpness was higher and optimal at the iodine accumulation on the surface area of the target than inside accumulation.

3. CONCLUSION

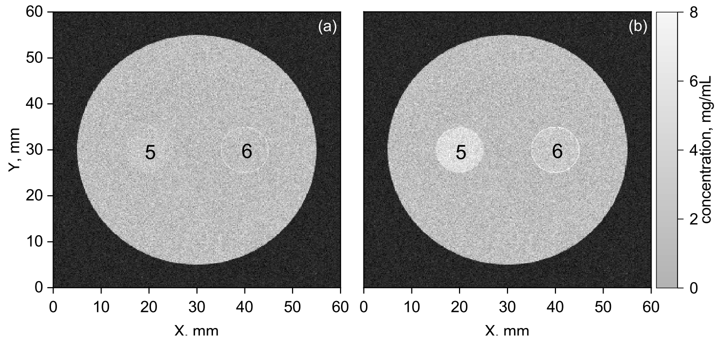

Fig. 5. X-ray images for different thickness of rod 5, 6 (a) 10 mm and (b) 50 mm with the same 8 mg/mL iodine concentration.

In this work, we demonstrated the effect of radio enhancement for X-ray imaging using some contrast media on the imaging phantom with different attenuation sites by a Monte Carlo method. The optimal contrast effect has been performed on the target with iodine at the 8.0 mg/mL concentration. The X-ray image with the iodine shell was brighter than uniform distribution due to increased iodine volume density for shorter targets. Finally, this study indicates the possibility of obtaining improved X-ray images for soft tissue (ICRP) in potential concentrations below the toxic limit of iodine inside a mammal.

REFERENCES

1. *Lusic, H., and Grinstaff, M. W.* X-ray-computed tomography contrast agents. // Chemical reviews — 2014. — V. 113(3). — P. 1641-1666.

2. *Prins, Marloes et al.* Pathological differences between white and grey matter multiple sclerosis lesions // Annals of the New York Academy of Sciences — 2015. — V. 1351. — P. 99-113. doi: 10.1111/nyas.12841

3. *Dawson P.* The non-ionic isotonic contrast agents. Perspectives and controversies // European radiology — 1996. — V. 6(2) — P. S20-4. — doi:10.1007/BF02342568

4. *Zeng, W. et al.* Safety of non-ionic contrast media in CT examinations for out-patients: retrospective multicenter analysis of 473,482 patients. // European radiology — 2024. — V. 34(9) — P. 5570–5577. — doi.org/10.1007/s00330-024-10654-2

5. *Baubeta, Erik et al.* No gadolinium K-edge detected on the first clinical photon-counting computed tomography scanner // Journal of Applied Clinical Medical Physics — 2024. — V. 25(4) — P. e14324. — DOI: 10.1002/acm2.14324

6. *Van der Molen, Aart J. et al.* Waiting times between examinations with intravascularly administered contrast media: a review of contrast media

pharmacokinetics and updated ESUR Contrast Media Safety Committee guidelines. // European radiology — 2024. — V. 34(4) — P. 2512–2523.

7. *Alsaihati, Njood et al.* Development, validation, and application of a generic image-based noise addition method for simulating reduced dose computed tomography images. // Medical Physics — 2022. — V. 32 — P. 34. — doi.org/10.1186/s40880-018-0299-7

8. *J. Valentin.* Basic anatomical and physiological data for use in radiological protection: reference values: ICRP Publication 89 // Annals of the ICRP 2002. — V. 32. — P. 1-277.

9. *Allison, John et al.* Recent developments in Geant4. // Nuclear instruments and methods in physics research section A: Accelerators, Spectrometers, Detectors and Associated Equipment — 2016. — V. 835. — P. 186–225.

10. *Poludniowski, Gavin et al.* SpekPy v2. 0—a software toolkit for modeling x-ray tube spectra. // Medical Physics — 2021. — V. 48(7). — P. 3630–3637.

11. *Tilley, Steven et al.* Model-based material decomposition with a penalized nonlinear least-squares CT reconstruction algorithm. // Physics in Medicine & Biology — 2019. — V. 64(3). — P. 035005.

12. *Steven Dolly.* Medical Physics Web Applications (https://solutioinsilico.com/medical-physics/applications/).